Zeitschrift für Angewandte Mathematik und Mechanik

# Granular micromechanics-based identification of isotropic strain gradient parameters for elastic geometrically nonlinear deformations



| | |
|---|---|
| Journal: | *Zeitschrift für Angewandte Mathematik und Mechanik* |
| Manuscript ID | zamm.202100059.R1 |
| Wiley - Manuscript type: | Original Paper |
| Date Submitted by the Author: | n/a |
| Complete List of Authors: | Barchiesi, Emilio; École Nationale d'Ingénieurs de Brest<br>Misra, Anil; University of Kansas, Civil, Environmental and Architectural Engineering Department<br>Placidi, Luca; International Telematic University Uninettuno, Engineering Faculty<br>Turco, Emilio; University of Sassari, Department of Architecture, Design and Urban planning |
| Keywords: | strain gradient, 2D continua, 3D continua, granular micromechanics, stiffness matrices |
| | |

# Granular micromechanics-based identification of isotropic strain gradient parameters for elastic geometrically nonlinear deformations

Emilio Barchiesi (1,2), Anil Misra (3), Luca Placidi (4), Emilio Turco (5)

April 21, 2021

(1) École Nationale d'Ingénieurs de Brest, ENIB, UMR CNRS 6027, IRDL, F-29200 Brest, France

(2) International Research Center on Mathematics and Mechanics of Complex Systems (M&MOCS), University of L'Aquila, Italy.

(3) The University of Kansas. Civil, Environmental and Architectural Engineering Department. 1530 W. 15th Street, Lawrence, KS 66045-7609 (USA).

(4) International Telematic University Uninettuno. Faculty of Engineering. Corresponding author: luca.placidi@uninettunouniversity.net.

(5) University of Sassari, Department of Architecture, Design and Urban planning (DADU), Italy.



**Abstract**

Although the primacy and utility of higher-gradient theories are being increasingly accepted, values of second gradient elastic parameters are not widely available due to lack of generally applicable methodologies. In this paper, we present such values for a second-gradient continuum. These values are obtained in the framework of finite deformations using granular micromechanics assumptions for materials that have granular textures at some 'microscopic' scale. The presented approach utilizes so-called Piola's ansatz for discrete-continuum identification. As a fundamental quantity of this approach, an objective relative displacement between grain-pairs is obtained and deformation energy of grain-pair is defined in terms of this measure. Expressions for elastic constants of a macroscopically linear second gradient continuum are obtained in terms of the micro-scale grain-pair parameters. Finally, the main result is that the same coefficients, both in the 2D and in the 3D cases, have been identified in terms of Young's modulus, of Poisson's ratio and of a microstructural length.

keywords: strain gradient, 2D continua, 3D continua, granular micromechanics, stiffness tensors

## 1 Introduction

Materials whose textural features can be described as granular at some 'microscopic' scale abound in all applications of science and engineering. Many of these materials are characterized by complexity and diversity of grain-scale mechano-morphology. Consequently, modeling approaches are needed that are both representative and tractable to describe their mechanical behavior. Continuum models, arguably, are the most feasible [6, 18, 23, 25]. However, these models must properly account for the granular nature of the material to be representative. To this end, it is notable that the deformation of materials with granular microstructures can be effectively described in terms of the relative movements of the grain centroids/barycenters regardless of the location of the actual deformation within the grains [62, 45]. The macro-scale deformation energy density of a volume of such material can then be described as an aggregation of grain-pair deformation energy and mathematically as

the sum of the deformation energy of all the grain pairs parameterized by the corresponding orientation. Elastic properties of materials with granular microstructures can, therefore, benefit from an identification between that of the grain-scale and the macro-scale (scales at which continuum representation is suitable). Such identification in the past has been focused upon linearized classical or Cauchy format of continuum mechanics theory in which infinitesimal strain is used as the measure of material deformation [63, 14, 32, 44] or for linearized Mindlin's third-gradient (second-strain gradient) theory [13, 42], and for linearized micromorphic continuum of degree 1 [46].

We further note that the use of strain gradient materials in the literature is not new [24, 25, 43, 49]. The theoretical investigation of second gradient materials [23, 24, 29] in the recent past are highlighted in [21, 40, 56] and have been complemented with preliminary identification procedures [25, 27] for specific microstructures. However, those constitutive coefficients that emerge to be relevant in such theories have not yet been experimentally identified [16, 17, 39, 54, 65]. The reason is that it is difficult to experimentally [11, 10, 48] apply proper boundary conditions, e.g. within the procedure investigated in [5, 50], that are necessary to perform such a characterization. Besides, in order to perform proper numerical simulations [2, 1, 55] the identification of second gradient constant is generally done with arbitrary (a priori) simplifications that are based, regardless of the investigated application of the model, on the sake of simplicity [4, 38, 64], although it is possible that for describing certain phenomena only a subset of characteristic lengths may be required [36].

In this connection, it is also useful to note that [15] studies an even higher-gradient (third-gradient of displacement) formulation for nano-objects. A formulation of the same order but with six non-classical stiffness parameters (three of them coupling strains and strain gradients of different orders) and two micro-inertia parameters has also been shown in [34]. Besides completing the stability analysis of [15], this formulation captures surface tension/compression effects and shear effects appearing in a plane lattice structures, that interestingly, are not nano-objects. The parameter identification, in these aforementioned works, is based upon parameter fitting via numerical experiments performed using fine-scale computational models (as surrogates to laboratory experiments with fine-scale physical samples). Further efforts at identification of higher-gradient constants are found in the works related to micro-architectural thin structures. For instance, to model the small-scale bending experiments of [38] and others, it has been shown that a single non-classical parameter is enough, in addition to the classical Young's modulus, for capturing size effects present in the bending of planar lattice metamaterial beam structures described by 1D generalized beam bending model for both linear ([33, 35]) and geometrically nonlinear [61] analyses. On the other hand, for modeling a 2D model discussed in [66] more that one non-classical parameters are needed although there is no clarity on the which of these are most relevant. Along these lines, it hase been shown in [36] (for linear) and [60] (for geometrically nonlinear), that at least four non-classical parameters are necessary for modeling the bending problem of cellular metamaterial plate structures. In contrast, a single non-classical parameter appears to be sufficient for modeling the bending of octet-truss beam structures as seen by the results of both numerical and physical experiments given in [37]. While it is clear that the problem-type and accuracy-requirements determine the need for classical or non-classical description and associated simplifications in terms of constitutive relations and model dimensionality (1D, 2D or 3D), such determination may not be possible *a priori,* and a general approach may be preferred.

In this work, we consider the identification of second gradient elastic constants in a more generalized setting of finite deformations of materials with granular textures. The implication of considering higher gradients for granular materials is that the deformation energy associated with grain-pair embedded in a system of grains is intrinsically linked to its extended neighborhood and cannot be estimated as that of a isolated grain-pair. It is notable that the grain-scale defromation mechanisms can be complex due to, for example, the grain-scale structure, presence of void spaces, grain rotations, and the wide contrast in the bulk grain stiffness and the typically compliant interactions [47, 53]. With this view as a point of departure, we utilize a variational approach for modeling the elastic behavior of granular solids under finite deformations based upon grain-pair interactions. Consequently, as a first step we develop an objective kinematic descriptor for grain-pair relative displacement in the framework of strain-gradient theory linked to the placement function in deformed configuration utilizing Piola's ansatz for micro-macro identification. We remark from view point of novelty that Piola's micro-macro kinematic identification utilized here provides a distinct pathway for continuum-discrete identification, which can admit not only higher-gradients but also

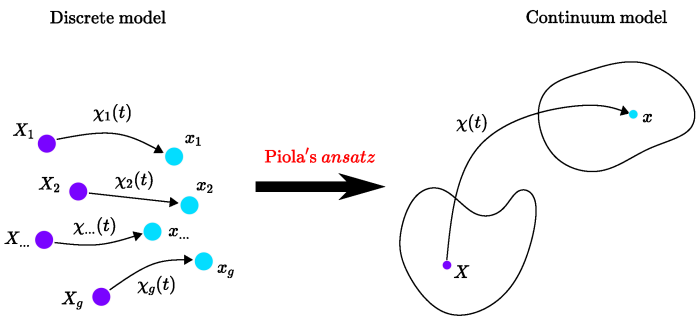


Figure 1: Piola's Ansatz. On the left a scheme with the kinematical descriptors of the discrete model. On the right a scheme with the kinematical descriptor of the continuum model.

additional kinematic measures that lead to higher-order descriptions (see for example [47]). Grain-pair deformation energy is then introduced in terms of the objective grain-pair relative displacement decomposed into a component along the vector joining the grain centroids of a grain-pair, termed as normal component, and a component in the orthogonal direction, termed as tangential component. For the present work, a quadratic form of the grain-pair deformation energy is utilized to obtain an identification for the case of linear isotropic elasticity. As a result, expressions for elastic constants of a macroscopically linear second gradient continuum are obtained in terms of the micro-scale grain-pair parameters. These expressions represent a first estimate of second-gradient linear elasticity that generalize those available in the literature. The main new result is that these coefficients have been identified in terms of (i) Young's modulus, (ii) Poisson's ratio and (iii) a microstructural length, that can be interpreted as the distance of the grain-pair. The aim of this paper is a first attempt to give a contribution in this regards. It is finally worth to be noted that this method could be applied also to those metamaterials, such as pantographic structures [9, 54, 31, 22, 20, 28, 51], for which a preliminary guess for the identification of its constitutive coefficients is necessary [19, 58].

# 2 Discrete and continuous models for granular systems

## 2.1 Piola's ansatz for the identification in space

Let us consider a discrete model consisting of $g$ grains. In the reference configuration the position of the $A$-th grain is given by $X_A \in E^{2,3}$ with $A = 1, \dots, g$, where $E^2$ (and $E^3$) is the Euclidean two (and three) dimensional space. The position $x_A$ in the present (or actual) configuration of the same grain is evaluated with the placement function $\chi_A(t) = X_A + u_A(t)$, where $u_A(t)$ is the displacement of the $A$-th grain and placement $\chi_A$ and displacement $u_A$ are both functions on time $t$. In the continuum model we have a continuous body $\mathfrak{B}$ which, in the reference configuration, is constituted by infinite particles having position $X$, i.e. $X \in \mathfrak{B}$. Each particle is placed, in the present (or actual) configuration with the placement function $\chi(X,t) = X + u(X,t)$, where $u(X,t)$ is the displacement function of the continuous body $\mathfrak{B}$.

In the continuum-discrete model's identification, the Piola's Ansatz

$$\chi(X_A,t) = \chi_A(t), \quad A = 1, \dots, g \tag{1}$$

holds, that means that the placement $\chi_A(t)$ of the $A$-th grain is equal to the placement $\chi(X_A,t)$ of the continuous body $\mathfrak{B}$ evaluated at the point $X = X_A$, where the grain is located in the reference configuration, see Fig. 1. We note that this kinematic identification is conceptually different from the Cauchy-Born type approximation often used in continuum-discrete identification (such as [59, 41]) and can admit additional kinematic measures that lead to higher-gradient descriptions as well as higher-order descriptions (a point that will be pursued in a forthcoming work).

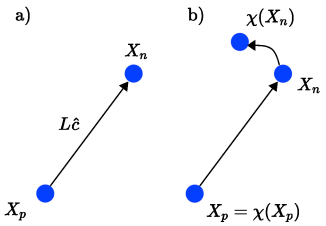


Figure 2: (a) On the left-hand side the reference configuration of the grain-pair. On the right-hand side the actual configuration of the grain pair under the rigid body rotation (6) centered at $X_p$.

## 2.2 Piola's ansatz in orientation as the homogenization rule

Let us assume that the distance between those grain at $X_n$ and $X_p$ is $L$ and the unit vector $\hat{c}$ is defined as follows,

$$X_n - X_p = \hat{c}L. \tag{2}$$

Let us consider the discrete model of $N$ grain-pairs of the $n-p$ type, all centered at the grain $p$ and each oriented as $\hat{c}$ towards one of the $N$ grains of the type $n$. Besides, let us be interested in a certain quantity $a_i$, for a given point$X_p$ and associated to the $i$-th grain-pair of the type $n-p$ oriented as $\hat{c}$. Thus, we assume the existence of a continuum function $a(\hat{c})$ with the following Piola's ansatz in the orientation space,

$$\int_{\mathcal{S}^{1,2}} a(\hat{c}) = \sum_{i=1}^{N} a_i, \tag{3}$$

where $\mathcal{S}^1$ is the unit circle, domain of the function $a(\hat{c})$ in the 2D case and where $\mathcal{S}^2$ is the unit sphere, domain of the function $a(\hat{c})$ in the 3D case. The homogenization rule made explicit in (3) means that the function $a(\hat{c})$ is, per unit element of $\mathcal{S}^1$ or of $\mathcal{S}^2$, equal to quantity $a_i$ associated to the $i$-th grain-pairs. This means to restrict the range of interest to those quantities $a_i$ that do not vary too much from a grain-pair oriented towards $\hat{c}$ to another grain-pair oriented towards an orientation in the neighboring of $\hat{c}$.

## 2.3 Relative intergranular displacement and related continuum deformation measures

In the reference configuration, therefore, the vector attached to the position $X_p$ and pointing the position $X_n$ is $\hat{c}L$ and given in (2), see also Fig. 2a. In the actual configuration the positions of the two grains at $X_n$ and $X_p$ are, respectively, $\chi(X_n,t)$ and $\chi(X_p,t)$. Thus, the vector in (2) in the actual configuration yields

$$\chi(X_n,t) - \chi(X_p,t). \tag{4}$$

The difference, at time $t$, between the vectors in (2) and (4) is called the relative displacement $\delta_{np}(t)$ of the two grains $n$ and $p$,

$$\delta_{np}(t) = \chi(X_n,t) - \chi(X_p,t) - (X_n - X_p) = u_n(t) - u_p(t). \tag{5}$$

It is a fundamental quantity in granular mechanics. However, it is not a measure for the deformation of the granular assembly (it is, e.g., not objective!). Indeed, a rigid body rotation centered e.g. at $X_p$,

$$x = \chi(X,t) = X_p + Q(X - X_p), \quad Q \in \mathrm{Orth}^+, \tag{6}$$

where $Orth^+$ is the orthogonal space of rotation, of the granular assembly (that should be associated to a null strain energy) yields both no displacement of the grain $p$

$$u_p(t) = \chi(X_p,t) - X_p = X_p + Q(X_p - X_p) - X_p = 0,$$

and, see also Fig.2b, a non-zero displacement for the grain $n$,

$$u_n(t) = \chi(X_n, t) - X_n = X_p + Q(X_n - X_p) - X_n = -\hat{c}L + LQ\hat{c}.$$

Thus, a non-zero relative displacement $\delta_{np}(t)$

$$\delta_{np}(t) = L[-I + Q]\hat{c} \neq 0,$$

where $I$ is the identity tensor.

In order to define an objective relative displacement (i.e. a relative displacement that is really a measure of the contribution of the $n-p$ pair to the deformation of the granular assembly), we proceed as follows. First we define the deformation gradient $F = \nabla\chi$ and its value $F_p$ evaluated at $X = X_p$ as the gradient of the placement function. Thus, we define an objective, see the analogy with eq. (5), relative displacement as

$$u^{np} = F_p^T(\chi(X_n, t) - \chi(X_p, t)) - (X_n - X_p). \tag{7}$$

The proof of the objectivity of the definition (7) is easy. Here, it is worth to be noted only that the rigid body rotation centered at $X_p$ according to (6) and to Fig. 2 yields an orthogonal deformation tensor $F = F_p = \nabla\chi = Q$ and therefore

$$u^{np} = Q^T(X_p + Q(X_n - X_p) - X_p) - (X_n - X_p) = Q^TQ(X_n - X_p) - (X_n - X_p) = 0,$$

that means that we have a null objective relative displacement for the rigid body rotation that is pictured in Fig. 2 and defined in (6).

Let us now assume that the two grains $n$ and $p$ are neighboring ones. Thus, they place similarly in the present configuration and the following Taylor's series expansion is possible

$$\chi(X_n) \cong \chi(X_p) + (\nabla\chi)_{X_p}(X_n - X_p) + \frac{1}{2}\left[(\nabla^2\chi)_{X_p}(X_p - X_n)\right](X_p - X_n). \tag{8}$$

The insertion of (2) and (8) into (7) yields

$$u^{np} = F^T\left(F\hat{c}L + \frac{1}{2}[\nabla F(\hat{c}L)](\hat{c}L)\right) - \hat{c}L = 2G\hat{c}L + \frac{1}{2}L^2[\nabla G\hat{c}]\hat{c} \tag{9}$$

where the deformation gradient $F$ as well as the Green-Saint-Venant tensor $G$ and its gradient

$$F = (\nabla\chi)_{X_p}, \quad G = \frac{1}{2}(F^TF - I), \quad \nabla G = F^T\nabla F, \tag{10}$$

have been defined and all evaluated at $X = X_p$.

The half-projection of the objective relative displacement on the unit vector $\hat{c}$, defined in (2), is the so called (scalar) normal displacement $u_\eta$,

$$u_\eta = \frac{1}{2}u^{np} \cdot \hat{c}, \tag{11}$$

where the reason of the $1/2$ will be clear in the Subsection 2.4. The projection-vector of the objective relative displacement that is tangent to $\hat{c}$ is the tangent displacement $u_\tau$,

$$u_\tau = u^{np} - (u^{np} \cdot \hat{c})\hat{c}. \tag{12}$$

## 2.4 Example

Let us assume a frame of reference $\{O, \hat{e}_1, \hat{e}_2, \hat{e}_3\}$ oriented with the grain pair direction $\hat{e}_2 = \hat{c}$ and with the origin in $p$ , i.e. $O = X_p$. Thus, the column $[X]$ is the representation, in the same frame of reference, of the position $X$ in the reference configuration,

$$[X] = \begin{pmatrix} X_1 \\ X_2 \\ X_3 \end{pmatrix}.$$

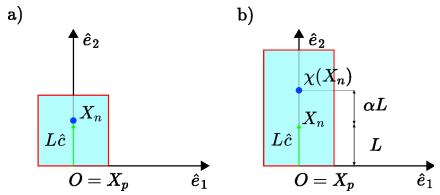


Figure 3: Vertical deformation of the $n-p$ grain pair. (a) Reference configuration of the granular assembly. (b) Actual configuration with a vertical elongation along the $n-p$ grain pair.

We first consider the state of tension along the horizontal direction $\hat{e}_1$ given by a placement function $\chi$ with the following column-representation

$$[\chi] = \begin{pmatrix} \chi_1 \\ \chi_2 \\ \chi_3 \end{pmatrix} = \begin{pmatrix} X_1 + \alpha X_1, \\ X_2 \\ X_3 \end{pmatrix}.$$

Keeping this in mind the deformation gradient $F$, the Green-Saint-Venant tensor $G$ and its gradient $\nabla G$ are

$$[F] = \begin{pmatrix} 1+\alpha & 0 & 0 \\ 0 & 1 & 0 \\ 0 & 0 & 1 \end{pmatrix}, \quad [G] = \begin{pmatrix} \alpha + \frac{1}{2}\alpha^2 & 0 & 0 \\ 0 & 0 & 0 \\ 0 & 0 & 0 \end{pmatrix}, \quad \nabla G = 0,$$

that yield a null objective relative displacement

$$[u^{np}] = 2L\,[G]\,[\hat{e}_2] = 2L \begin{pmatrix} \alpha + \frac{1}{2}\alpha^2 & 0 & 0 \\ 0 & 0 & 0 \\ 0 & 0 & 0 \end{pmatrix} \begin{pmatrix} 0 \\ 1 \\ 0 \end{pmatrix} = \begin{pmatrix} 0 \\ 0 \\ 0 \end{pmatrix}$$

and the corresponding normal and tangent measures are also null, i.e.,

$$u_\eta = \frac{1}{2}\,[u^{np}]^T \cdot [\hat{e}_2] = \frac{1}{2} \begin{pmatrix} 0 & 0 & 0 \end{pmatrix} \cdot \begin{pmatrix} 0 \\ 1 \\ 0 \end{pmatrix} = 0, \quad [u_\tau] = [u^{np}] - \left([u^{np}]^T \cdot [\hat{e}_2]\right)[\hat{e}_2] = \begin{pmatrix} 0 \\ 0 \\ 0 \end{pmatrix},$$

where the transpose symbol $T$ is used in compliance with the rows by columns rules. It is a matter of fact that also the relative displacement $\delta_{np} = 0$ is null because the displacements of the grains $n$ and $p$, are null as well, i.e.$u_n = 0$ and $u_p = 0$.

We now consider a state of tension along the vertical direction $\hat{e}_2 = \hat{c}$ given by a placement function $\chi$ in Fig. 3 with the following column-representation

$$[\chi] = \begin{pmatrix} \chi_1 \\ \chi_2 \\ \chi_3 \end{pmatrix} = \begin{pmatrix} X_1, \\ X_2 + \alpha X_2 \\ X_3 \end{pmatrix}.$$

Keeping this in mind the deformation gradient $F$, the Green-Saint-Venant tensor $G$ and its gradient $\nabla G$ are

$$[F] = \begin{pmatrix} 1 & 0 & 0 \\ 0 & 1+\alpha & 0 \\ 0 & 0 & 1 \end{pmatrix}, \quad [G] = \begin{pmatrix} 0 & 0 & 0 \\ 0 & \alpha + \frac{1}{2}\alpha^2 & 0 \\ 0 & 0 & 0 \end{pmatrix}, \quad \nabla G = 0,$$

that yield a non-zero objective relative displacement,

$$[u^{np}] = 2\,[G]\,[\hat{e}_2]\,L = 2L \begin{pmatrix} 0 & 0 & 0 \\ 0 & \alpha + \frac{1}{2}\alpha^2 & 0 \\ 0 & 0 & 0 \end{pmatrix} \begin{pmatrix} 0 \\ 1 \\ 0 \end{pmatrix} = \begin{pmatrix} 0 \\ 2L\alpha + L\alpha^2 \\ 0 \end{pmatrix}$$

and the corresponding normal and tangent measures are

$$u_\eta = \frac{1}{2}\,[u^{np}]^T \cdot [\hat{e}_2] = L\alpha + \frac{1}{2}L\alpha^2,$$

$$[u_\tau] = [u^{np}] - \left([u^{np}]^T \cdot [\hat{e}_2]\right)[\hat{e}_2] = \begin{pmatrix} 0 \\ 2L\alpha + L\alpha^2 \\ 0 \end{pmatrix} - \left(2L\alpha + L\alpha^2\right) \begin{pmatrix} 0 \\ 1 \\ 0 \end{pmatrix} = \begin{pmatrix} 0 \\ 0 \\ 0 \end{pmatrix}.$$

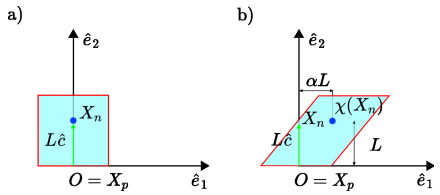


Figure 4: Shear deformation of the $n-p$ grain pair. (a) Reference configuration of the granular assembly. (b) Actual configuration with a shear orthogonal to the $n-p$ grain pair.

Besides the relative displacement $\delta_{np}$ is

$$[\delta_{np}] = [u_n] - [u_p] = \begin{pmatrix} 0 \\ L\alpha \\ 0 \end{pmatrix} - \begin{pmatrix} 0 \\ 0 \\ 0 \end{pmatrix} = \begin{pmatrix} 0 \\ L\alpha \\ 0 \end{pmatrix}$$

It is worth to be noted that for small deformation the normal displacement is equivalent to the vertical component of the relative displacement, i.e. $u_\eta \cong \delta_{np} \cdot \hat{e}_2 = L\alpha$, that justifies the presence of the factor $1/2$ in the definition (11).

Further, a state of shear displaced along the horizontal direction $\hat{e}_1$ is given by a placement function $\chi$ in Fig. 4 with the following column-representation

$$[\chi] = \begin{pmatrix} \chi_1 \\ \chi_2 \\ \chi_3 \end{pmatrix} = \begin{pmatrix} X_1 + \alpha X_2 \\ X_2 \\ X_3 \end{pmatrix}.$$

Keeping this in mind the deformation gradient $F$, the Green-Saint-Venant tensor $G$ and its gradient $\nabla G$ are

$$[F] = \begin{pmatrix} 1 & \alpha & 0 \\ 0 & 1 & 0 \\ 0 & 0 & 1 \end{pmatrix}, \quad [G] = \frac{1}{2}\begin{pmatrix} 0 & \alpha & 0 \\ \alpha & \alpha^2 & 0 \\ 0 & 0 & 0 \end{pmatrix}, \quad \nabla G = 0,$$

that yield a non-zero objective relative displacement,

$$[u^{np}] = 2\,[G]\,[\hat{e}_2]\,L = L\begin{pmatrix} 0 & \alpha & 0 \\ \alpha & \alpha^2 & 0 \\ 0 & 0 & 0 \end{pmatrix}\begin{pmatrix} 0 \\ 1 \\ 0 \end{pmatrix} = L\begin{pmatrix} \alpha \\ \alpha^2 \\ 0 \end{pmatrix}$$

and the corresponding normal and tangent measures are

$$u_\eta = \frac{1}{2}\,[u^{np}]^T \cdot [\hat{e}_2] = \frac{1}{2}L\alpha^2,$$

$$[u_\tau] = [u^{np}] - \left([u^{np}]^T \cdot [\hat{e}_2]\right)[\hat{e}_2] = L\begin{pmatrix} \alpha \\ \alpha^2 \\ 0 \end{pmatrix} - L\alpha^2\begin{pmatrix} 0 \\ 1 \\ 0 \end{pmatrix} = L\begin{pmatrix} \alpha \\ 0 \\ 0 \end{pmatrix}.$$

Besides the relative displacement $\delta_{np}$ is

$$[\delta_{np}] = [u_n] - [u_p] = \begin{pmatrix} L\alpha \\ 0 \\ 0 \end{pmatrix} - \begin{pmatrix} 0 \\ 0 \\ 0 \end{pmatrix} = \begin{pmatrix} L\alpha \\ 0 \\ 0 \end{pmatrix}$$

It is worth to be noted that for small deformation the normal displacement is null and therefore equivalent to the vertical component of the relative displacement, i.e. $u_\eta \cong \delta_{np} \cdot \hat{e}_2 = 0$. Besides, the tangent displacement $u_\tau$, as expected, correspond to the relative displacement $\delta_{np}$, i.e. $u_\tau = \delta_{np}$.

# 3 Elastic energy function

## 3.1 Elastic energy per unit volume for a grain-pair

The elastic energy per unit volume for a given grain-pair, say the pair $n-p$ considered in Section 2.3, $U_{np}$ is assumed to be a quadratic form of normal and tangent relative displacement,

$$U_{np} = \frac{1}{2}k_\eta u_\eta^2 + \frac{1}{2}k_\tau \left|u_\tau\right|^2, \tag{13}$$

where $u_\eta^2$ is the square of the scalar $u_\eta$, $|u_\tau|^2$ is the squared module of the vector $u_\tau$, $k_\eta$ is the normal stiffness associated to the normal displacement $u_\eta$ and $k_\tau$ is the tangent stiffness associated to the tangent displacement $u_\tau$. The elastic energy per unit volume is a scalar and therefore, for objectivity reasons, no coupling term between the scalar $u_\eta$ and the vector $u_\tau$ is admissible. The quadratic assumption in (13) is the easiest possible that represents linear elastic behavior of granular systems, however, it is not the unique option. Others, such as Lennard-Jones-type potential could be used that present asymmetry of tension-compression response which could lead to nonlinear elasticity with evolving anisotropy and chirality when subjected to loading.

## 3.2 Elastic energy per unit volume related to the grain at $X_p$

The elastic energy per unit volume $U_p$ for a given grain at $X_p$ is the sum of the energy per unit volume in (13) over all the $N$ possible interactions, i.e. between the grain $p$ and all the $N$ neighboring grains $n$,

$$U_p = \sum_{n=1}^{N} U_{np} = \sum_{i=1}^{N}\left[\frac{1}{2}k_{\eta i}u_{\eta i}^2 + \frac{1}{2}k_{\tau i}\left|u_{\tau i}\right|^2\right], \tag{14}$$

where the subscript $i$ refers to a single grain-pair of the type $n-p$. In (14) it is therefore intended that $k_{\eta i}$, $k_{\tau i}$, $u_{\eta i}$ and $u_{\tau i}$ are the normal stiffness, the tangent stiffness, the scalar normal displacement and the vector tangent displacement all associated for the $i$-th grain-pair of the type $n-p$.

## 3.3 Continuum approximation in the orientation space

The use of the Piola's ansatz in (3) for the energy per unit volume in (14) yields

$$U_p = \int_{\mathcal{S}^{1,2}} \frac{1}{2}k_\eta u_\eta^2 + \frac{1}{2}k_\tau \left|u_\tau\right|^2, \tag{15}$$

where $k_\eta = \widetilde{k}_\eta(\hat{c})$ and $k_\tau = \widetilde{k}_\tau(\hat{c})$ substitute, respectively, $k_{\eta i}$ $k_{\tau i}$ and are all functions of that orientation $\hat{c}$. As we have already pointed out at the end of Subsection 2.2, we are assuming that the stiffnesses $k_{\eta i}$ and $k_{\tau i}$ do not vary too much from a grain-pair oriented towards $\hat{c}_i$ to another grain-pair oriented towards an orientation in the neighboring of $\hat{c}_i$.

Insertion of (11) and (12) into the elastic energy per unit volume $U_p$ in (15), see the Appendix 6.1, yields the following expression in index notation

$$\begin{aligned}
U = &\int_{\mathcal{S}^{1,2}} \frac{1}{2}k_\eta \left(L^2\hat{c}_i\hat{c}_j\hat{c}_a\hat{c}_b G_{ij}G_{ab} + \frac{1}{2}L^3\hat{c}_i\hat{c}_j\hat{c}_a\hat{c}_b\hat{c}_c G_{ij}G_{ab,c}\right)\\
&\int_{\mathcal{S}^{1,2}} \frac{1}{2}k_\eta \left(\frac{1}{16}L^4\hat{c}_i\hat{c}_j\hat{c}_h\hat{c}_a\hat{c}_b\hat{c}_c G_{ij,h}G_{ab,c}\right)\\
&+\int_{\mathcal{S}^{1,2}} \frac{1}{2}k_\tau \left(4L^2 G_{ij}G_{ab}\left(\delta_{ia}\hat{c}_j\hat{c}_b - \hat{c}_i\hat{c}_j\hat{c}_a\hat{c}_b\right) + 2L^3 G_{ij}G_{ab,c}\left(\delta_{ia}\hat{c}_j\hat{c}_b\hat{c}_c - \hat{c}_i\hat{c}_j\hat{c}_a\hat{c}_b\hat{c}_c\right)\right)\\
&+\int_{\mathcal{S}^{1,2}} \frac{1}{2}k_\tau \left(\frac{1}{4}L^4 G_{ij,h}G_{am,n}\left(\delta_{ia}\hat{c}_j\hat{c}_h\hat{c}_m\hat{c}_n - \hat{c}_i\hat{c}_j\hat{c}_h\hat{c}_a\hat{c}_b\hat{c}_c\right)\right),
\end{aligned} \tag{16}$$

where from now on we omit the subscript $p$. Eq. (16) yield, in a compact form,

$$U = \frac{1}{2}\mathbb{C}_{ijab}G_{ij}G_{ab} + \mathbb{M}_{ijabc}G_{ij}G_{ab,c} + \frac{1}{2}\mathbb{D}_{ijhabc}G_{ij,h}G_{ab,c}, \tag{17}$$

where the elastic stiffness $\mathbb{C}$, $\mathbb{M}$ and $\mathbb{D}$, are identified in (17) as follows, with the symmetrization induced by the symmetry of the strain tensor $G$,

$$\mathbb{C}_{ijab} = L^2 \int_{\mathcal{S}^{1,2}} k_\eta \hat{c}_i \hat{c}_j \hat{c}_a \hat{c}_b \tag{18}$$
$$+L^2 \int_{\mathcal{S}^{1,2}} k_\tau \left( (\delta_{ia}\hat{c}_j\hat{c}_b + \delta_{ib}\hat{c}_j\hat{c}_a + \delta_{ja}\hat{c}_i\hat{c}_b + \delta_{jb}\hat{c}_i\hat{c}_a) - 4\hat{c}_i\hat{c}_j\hat{c}_a\hat{c}_b \right)$$
$$\mathbb{M}_{ijabc} = \frac{1}{4} L^3 \int_{\mathcal{S}^{1,2}} k_\eta \hat{c}_i \hat{c}_j \hat{c}_a \hat{c}_b \hat{c}_c \tag{19}$$
$$+\frac{L^3}{4} \int_{\mathcal{S}^{1,2}} k_\tau \left( (\delta_{ia}\hat{c}_j\hat{c}_b + \delta_{ib}\hat{c}_j\hat{c}_a + \delta_{ja}\hat{c}_i\hat{c}_b + \delta_{jb}\hat{c}_i\hat{c}_a)\, \hat{c}_c - 4\hat{c}_i\hat{c}_j\hat{c}_a\hat{c}_b\hat{c}_c \right)$$
$$\mathbb{D}_{ijhabc} = \frac{1}{16} L^4 \int_{\mathcal{S}^{1,2}} k_\eta \hat{c}_i \hat{c}_j \hat{c}_h \hat{c}_a \hat{c}_b \hat{c}_c \tag{20}$$
$$+\frac{L^4}{16} \int_{\mathcal{S}^{1,2}} k_\tau \left( (\delta_{ia}\hat{c}_j\hat{c}_b + \delta_{ib}\hat{c}_j\hat{c}_a + \delta_{ja}\hat{c}_i\hat{c}_b + \delta_{jb}\hat{c}_i\hat{c}_a)\, \hat{c}_h\hat{c}_c - 4\hat{c}_i\hat{c}_j\hat{c}_h\hat{c}_a\hat{c}_b\hat{c}_c \right).$$

# 4 Identification of the isotropic case

## 4.1 Macroscopic elastic constants in 2D and in 3D cases

Isotropic standard representation of the 4th order stiffness tensor for both 2D and 3D cases is

$$\mathbb{C}_{ijab} = \mu\delta_{ia}\delta_{jb} + \mu\delta_{ib}\delta_{ja} + \lambda\delta_{ij}\delta_{ab}, \tag{21}$$

where $\lambda$ and $\mu$ are the 2D or 3D Lamè coefficients. Thus, it is sufficient to know the following two components of $\mathbb{C}$,

$$\mathbb{C}_{1111} = \lambda + 2\mu, \qquad \mathbb{C}_{1122} = \lambda, \tag{22}$$

to identify Lamè coefficients as follows

$$\lambda = \mathbb{C}_{1122}, \qquad \mu = \frac{1}{2}\left(\mathbb{C}_{1111} - \mathbb{C}_{1122}\right). \tag{23}$$

Besides, the 4 independent strain gradient isotropic elastic coefficients in the 2D case are here reported in the nomenclature of [7], i.e.,

$$a_{11} = \mathbb{D}_{111111}, \quad a_{22} = \mathbb{D}_{221221}, \quad a_{12} = \mathbb{D}_{111221}, \quad a_{23} = \sqrt{2}\mathbb{D}_{221122}. \tag{24}$$

Finally, for the 3D case, the isotropic representation of the strain gradient elasticity stiffness tensor is

$$\mathbb{D}_{ijklmn} = c_3\left(\delta_{ij}\delta_{kl}\delta_{mn} + \delta_{in}\delta_{jk}\delta_{lm} + \delta_{ij}\delta_{km}\delta_{ln} + \delta_{ik}\delta_{jn}\delta_{lm}\right) \tag{25}$$
$$+c_4\delta_{ij}\delta_{kn}\delta_{ml}$$
$$+c_5\left(\delta_{ik}\delta_{jl}\delta_{mn} + \delta_{im}\delta_{jk}\delta_{ln} + \delta_{ik}\delta_{jm}\delta_{ln} + \delta_{il}\delta_{jk}\delta_{mn}\right)$$
$$+c_6\left(\delta_{il}\delta_{jm}\delta_{kn} + \delta_{im}\delta_{jl}\delta_{kn}\right)$$
$$+c_7\left(\delta_{il}\delta_{jn}\delta_{mk} + \delta_{im}\delta_{jn}\delta_{lk} + \delta_{in}\delta_{jl}\delta_{km} + \delta_{in}\delta_{jm}\delta_{kl}\right)$$

Thus, it is sufficient to know the following five components of $\mathbb{D}$,

$$\mathbb{D}_{111111} = 4c_3 + c_4 + 4c_5 + 2c_6 + 4c_7, \quad \mathbb{D}_{221221} = c_4 + 2c_6, \tag{26}$$
$$\mathbb{D}_{111221} = 2c_3 + c_4, \quad \mathbb{D}_{221122} = c_3 + 2c_7, \quad \mathbb{D}_{112223} = c_3, \tag{27}$$

to identify the five independent isotropic strain gradient coefficients as follows,

$$c_3 = \mathbb{D}_{112223}, \quad c_4 = \mathbb{D}_{111221} - 2\mathbb{D}_{112223}, \quad c_5 = \frac{1}{4}\left(\mathbb{D}_{111111} - 2\mathbb{D}_{112223} - 2\mathbb{D}_{221122} - \mathbb{D}_{221221}\right),$$
$$c_6 = \frac{1}{2}\left(2\mathbb{D}_{112223} + \mathbb{D}_{221221} - \mathbb{D}_{111221}\right), \quad c_7 = \frac{1}{2}\left(\mathbb{D}_{221122} - \mathbb{D}_{112223}\right)$$

Finally, we remark that in the isotropic case we have identically that $\mathbb{M} = 0$ for the assumed quadratic form of the grain-pair deformation energy.

Thus, it is straightforward to show that insertion of $\mathbb{M} = 0$, (21) and (25) into (17) yields,

$$U = \mu G_{ij} G_{ij} + \frac{1}{2}\lambda G_{ii} G_{jj} + 2c_3 G_{ii,j} G_{jh,h} + \frac{1}{2} c_4 G_{ii,k} G_{ll,k} \\ + 2c_5 G_{ij,i} G_{jm,m} + c_6 G_{ij,k} G_{ij,k} + 2c_7 G_{ij,k} G_{ki,j}$$

and, comparing with eq. (2.5) and with the fifth definition of (1.1) of Mindlin and Eshel 1968 [43], we have the following identities,

$$\hat{a}_1 = 2c_3, \quad \hat{a}_2 = \frac{c_4}{4}, \quad \hat{a}_3 = 2c_5, \quad \hat{a}_4 = c_6, \quad \hat{a}_5 = 2c_7. \tag{28}$$

## 4.2 Elastic constants in the 2D case in terms of micro-stiffness

In the 2D case, a standard representation of the unit vector $\hat{c}$ is

$$\hat{c}_1 = \cos\theta, \ \hat{c}_2 = \sin\theta, \tag{29}$$

where $\theta$ is the anti-clockwise angle from the first unit vector $\hat{e}_1$ of the frame of reference to $\hat{n}$. The components $\mathbb{C}_{1111}$, $\mathbb{C}_{1122}$, $\mathbb{D}_{111111}, \mathbb{D}_{221221}, \mathbb{D}_{111221}, \mathbb{D}_{221122}$, are, from (18), (20) and (29),

$$\mathbb{C}_{1111} = L^2 \int_0^{2\pi} \left[ \widetilde{k}_\eta(\theta) \cos^4\theta + 4\widetilde{k}_\tau(\theta) \left(\cos^2\theta - \cos^4\theta\right) \right] = \frac{L^2}{4}\left(3\bar{k}_\eta + 4\bar{k}_\tau\right) \tag{30}$$

$$\mathbb{C}_{1122} = L^2 \int_0^{2\pi} \left[ \widetilde{k}_\eta(\theta) \sin^2\theta\cos^2\theta + 4\widetilde{k}_\tau(\theta) \left(-\sin^2\theta\cos^2\theta\right) \right] = \frac{L^2}{8}\left(\bar{k}_\eta - 4\bar{k}_\tau\right), \tag{31}$$

$$\mathbb{D}_{111111} = \frac{L^4}{4} \int_0^{2\pi} \left[ \frac{1}{4}\widetilde{k}_\eta(\theta) \cos^6\theta + \widetilde{k}_\tau(\theta) \left(\cos^4\theta - \cos^6\theta\right) \right] = \frac{L^4}{256}\left[5\bar{k}_\eta + 4\bar{k}_\tau\right] \tag{32}$$

$$\mathbb{D}_{221221} = \frac{L^4}{4} \int_0^{2\pi} \left[ \frac{1}{4}\widetilde{k}_\eta(\theta) \sin^4\theta\cos^2\theta + \widetilde{k}_\tau(\theta) \left(\sin^2\theta\cos^2\theta - \sin^4\theta\cos^2\theta\right) \right] \tag{33}$$

$$= \frac{L^4}{256}\left[\bar{k}_\eta + 4\bar{k}_\tau\right] \tag{34}$$

$$\mathbb{D}_{111221} = \frac{L^4}{4} \int_0^{2\pi} \left[ \frac{1}{4}\widetilde{k}_\eta(\theta) \sin^2\theta\cos^4\theta + \widetilde{k}_\tau(\theta) \left(-\sin^2\theta\cos^4\theta\right) \right] = \frac{L^4}{256}\left[\bar{k}_\eta - 4\bar{k}_\tau\right] \tag{35}$$

$$\mathbb{D}_{221122} = \frac{L^4}{4} \int_0^{2\pi} \left[ \frac{1}{4}\widetilde{k}_\eta(\theta) \sin^4\theta\cos^2\theta + \widetilde{k}_\tau(\theta) \left(\frac{1}{2}\sin^2\theta\cos^2\theta - \sin^4\theta\cos^2\theta\right) \right] = \frac{L^4}{256}\bar{k}_\eta \tag{36}$$

where the isotropic condition has been imposed by assuming no dependence of $k_\eta$ and $k_\tau$ with respect to $\hat{c}$ (or to $\theta$),

$$\widetilde{k}_\eta(\theta) = \frac{\bar{k}_\eta}{2\pi}, \qquad \widetilde{k}_\tau(\theta) = \frac{\bar{k}_\tau}{2\pi},$$

where $\bar{k}_\eta$ and $\bar{k}_\tau$ are the integrated stiffness over the set of possible orientations, that are defined in the general anisotropic case as follows,

$$\bar{k}_\eta = \int_0^{2\pi} \widetilde{k}_\eta(\theta)\, d\theta, \qquad \bar{k}_\tau = \int_0^{2\pi} \widetilde{k}_\tau(\theta)\, d\theta.$$

It is worth to be noted that positive definiteness of the elastic energy per unit volume for a given grain-pair in (13) is, from (65) and (67) and neglecting the strain gradient contribution

$$U_{np} = \frac{1}{2}k_\eta u_\eta^2 + \frac{1}{2}k_\tau |u_\tau|^2 = \frac{1}{2}k_\eta L^2 \hat{c}_i\hat{c}_j\hat{c}_a\hat{c}_b G_{ij}G_{ab} + \frac{1}{2}k_\tau 4L^2 G_{ij}G_{ab}\left(\delta_{ia}\hat{c}_j\hat{c}_b - \hat{c}_i\hat{c}_j\hat{c}_a\hat{c}_b\right), \tag{37}$$

that is a quadratic form of $G_{11}$, $G_{12} = G_{21}$ and $G_{22}$. The number of eigenvalues of the Hessian of such a quadratic form, with the insertion of (29), are found to be three. One of the eigenvalue is null $\lambda_3 = 0$ and the other two $\lambda_{1,2}$ are

$$\lambda_{1,2} = \frac{1}{4}\left[ f(k_\eta, k_\tau, x) \pm \sqrt{\left[f(k_\eta, k_\tau, x)\right]^2 - g(k_\eta, k_\tau, x)} \right]$$

where

$$f\left(k_\eta, k_\tau, x=\cos 4\theta\right) = k_\eta\left(5-x\right) + 4k_\tau\left(3+x\right), \quad g\left(k_\eta, k_\tau, x=\cos 4\theta\right) = 32k_\eta k_\tau\left(7+x\right).$$

In order to have both non-zero eigenvalues to be positive, we have

$$k_\eta > 0, \qquad k_\tau > 0. \tag{38}$$

### 4.3 Isotropic micro-macro identification for the 2D case

By comparing (23), (30) and (31), we obtain the following identification of the 2D Lamè coefficients in terms of normal and tangent stiffness

$$\mu = \frac{L^2}{8}\left(\bar{k}_\eta + 4\bar{k}_\tau\right), \qquad \lambda = \frac{L^2}{8}\left(\bar{k}_\eta - 4\bar{k}_\tau\right). \tag{39}$$

In the 2D model, Young's modulus $Y_{2D}$ and Poisson's ratio $\nu_{2D}$ are derived in the Appendix 6.2.1 and in (74), i.e.,

$$Y_{2D} = 4\mu\frac{\lambda+\mu}{\lambda+2\mu}, \quad \nu_{2D} = \frac{\lambda}{\lambda+2\mu}, \tag{40}$$

Thus, insertion of (39) into (40) yield an identification of $2D$ Young's modulus and Poisson's ratio in terms of integrated stiffness $\bar{k}_\eta$ and $\bar{k}_\tau$ as follows,

$$Y_{2D} = L^2\bar{k}_\eta\frac{\bar{k}_\eta + 4\bar{k}_\tau}{3\bar{k}_\eta + 4\bar{k}_\tau}, \quad \nu_{2D} = \frac{\bar{k}_\eta - 4\bar{k}_\tau}{3\bar{k}_\eta + 4\bar{k}_\tau} \tag{41}$$

The inversion of (41) is

$$\bar{k}_\eta = \frac{2Y_{2D}}{L^2\left(1-\nu_{2D}\right)}, \quad \bar{k}_\tau = \frac{Y_{2D}\left(1-3\nu_{2D}\right)}{2L^2\left(1-\nu_{2D}\right)\left(1+\nu_{2D}\right)}. \tag{42}$$

Positive definiteness condition in (38) implies the following

$$Y_{2D} > 0, \qquad \nu_{2D} \in \left(-1, \frac{1}{3}\right).$$

By comparing (24), (32), (33), (35) and (36), we obtain the following identification of the four $2D$ strain gradient coefficients in terms of normal and tangent stiffness,

$$a_{11} = \frac{L^4}{256}\left[5\bar{k}_\eta + 4\bar{k}_\tau\right], \quad a_{22} = \frac{L^4}{256}\left[\bar{k}_\eta + 4\bar{k}_\tau\right], \quad a_{12} = \frac{L^4}{256}\left[\bar{k}_\eta - 4\bar{k}_\tau\right], \quad a_{23} = \frac{\sqrt{2}L^4}{256}\bar{k}_\eta. \tag{43}$$

or, by insertion (42) into (43), we have an identification of the 4 2D isotropic strain gradient stiffnesses not only in terms of the characteristic length $L$ but also in terms of $2D$ Young's modulus and Poisson's ratio

$$a_{11} = Y_{2D}L^2\frac{3+\nu_{2D}}{\left(1-\nu_{2D}\right)\left(1+\nu_{2D}\right)}, \quad a_{22} = Y_{2D}L^2\frac{1}{64\left(1+\nu_{2D}\right)}, \tag{44}$$

$$a_{12} = Y_{2D}L^2\frac{\nu_{2D}}{32\left(1-\nu_{2D}\right)}, \quad a_{23} = Y_{2D}L^2\frac{\sqrt{2}}{128\left(1-\nu_{2D}\right)}. \tag{45}$$

### 4.4 Elastic constants in the 3D case in terms micro-stiffness

In the $3D$ case, a standard representation of the unit vector $\hat{c}$ is

$$\hat{c}_1 = \cos\varphi\sin\theta, \ \hat{c}_2 = \sin\varphi\sin\theta, \ \hat{c}_3 = \cos\theta, \tag{46}$$

where $\varphi$ and $\theta$ are the longitude (the angle from the unit vector $\hat{e}_1$ to the projection of $\hat{c}$ on the plane generated by $\hat{e}_1$ and $\hat{e}_2$) and co-latitude (the angle from the unit vector $\hat{e}_3$ to $\hat{c}$), respectively,

of the unit sphere $S^2$. The stiffness tensor $\mathbb{C}$ in the $3D$ case is the same of (18) but the integral is extended to the unit sphere $S^2$

$$\mathbb{C}_{ijab} = 4L^2 \int_{\mathcal{S}^2} \left[ k_\eta \hat{c}_i \hat{c}_j \hat{c}_a \hat{c}_b + k_\tau \left( \delta_{ia} \hat{c}_j \hat{c}_b - \hat{c}_i \hat{c}_j \hat{c}_a \hat{c}_b \right) \right], \tag{47}$$

so that the components $\mathbb{C}_{1111}$ and $\mathbb{C}_{1122}$ are, from (47) and (46),

$$\mathbb{C}_{1111} = 4L^2 \int_0^\pi \sin\theta \left\{ \int_0^{2\pi} \left[ \left( k_\eta(\theta,\varphi) - k_\tau(\theta,\varphi) \right) \cos^4\varphi \sin^4\theta + k_\tau(\theta,\varphi) \cos^2\varphi \sin^2\theta \right] d\varphi \right\} d\theta \tag{48}$$

$$= \frac{4}{15} L^2 \left[ \frac{3}{4} \bar{k}_\eta + 2\bar{k}_\tau \right] \tag{49}$$

$$\mathbb{C}_{1122} = 4L^2 \int_0^\pi \sin\theta \left\{ \int_0^{2\pi} \left[ \sin^2\varphi \cos^2\varphi \sin^4\theta \right] \left( \frac{1}{4} k_\eta(\theta,\varphi) - k_\tau(\theta,\varphi) \right) d\varphi \right\} d\theta = \tag{50}$$

$$= \frac{4}{15} L^2 \left[ \frac{3}{4} \bar{k}_\eta + 2\bar{k}_\tau \right] \tag{51}$$

The strain gradient stiffness tensor in the 3D case is the same of (20) but the integral is extended to the unit sphere $S^2$

$$\mathbb{D}_{ijhabc} = \frac{1}{16} L^4 \int_{\mathcal{S}^2} k_\eta \hat{c}_i \hat{c}_j \hat{c}_h \hat{c}_a \hat{c}_b \hat{c}_c$$
$$+ \frac{1}{4} L^4 \int_{\mathcal{S}^2} k_\tau \left( \frac{1}{4} \left( \delta_{ia} \hat{c}_j \hat{c}_b + \delta_{ib} \hat{c}_j \hat{c}_a + \delta_{ja} \hat{c}_i \hat{c}_b + \delta_{jb} \hat{c}_i \hat{c}_a \right) \hat{c}_h \hat{c}_c - \hat{c}_i \hat{c}_j \hat{c}_h \hat{c}_a \hat{c}_b \hat{c}_c \right)$$

The 5 independent components in (26) and (27)

$$\mathbb{D}_{111111} = \frac{1}{4} L^4 \int_0^\pi \sin\theta \left\{ \int_0^{2\pi} \left[ \left[ \frac{1}{4} k_\eta(\theta,\varphi) - k_\tau(\theta,\varphi) \right] \cos^6\varphi \sin^6\theta \right] d\varphi \right\} d\theta$$
$$+ \frac{1}{4} L^4 \int_0^\pi \sin\theta \left\{ \int_0^{2\pi} \left[ k_\tau(\theta,\varphi) \left[ \cos^4\varphi \sin^4\theta \right] \right] d\varphi \right\} d\theta =$$
$$\mathbb{D}_{111111} = \frac{1}{140} L^4 \left( \frac{5}{4} \bar{k}_\eta + 2\bar{k}_\tau \right) \tag{52}$$

$$\mathbb{D}_{221221} = \frac{1}{4} L^4 \int_0^\pi \sin\theta \left\{ \int_0^{2\pi} \left[ \left[ \frac{1}{4} k_\eta(\theta,\varphi) - k_\tau(\theta,\varphi) \right] \cos^2\varphi \sin^4\varphi \sin^6\theta \right] d\varphi \right\} d\theta$$
$$+ \frac{1}{4} L^4 \int_0^\pi \sin\theta \left\{ \int_0^{2\pi} \left[ k_\tau(\theta,\varphi) \frac{1}{4} \left[ 4 \left( \sin^4\theta \sin^4\varphi \right) \cos^2\varphi \sin^2\theta \right] \right] d\varphi \right\} d\theta =$$
$$\mathbb{D}_{221221} = \frac{1}{420} L^4 \left( \frac{3}{4} \bar{k}_\eta + 4\bar{k}_\tau \right) \tag{53}$$

$$\mathbb{D}_{111221} = \frac{1}{4} L^4 \int_0^\pi \sin\theta \left\{ \int_0^{2\pi} \left[ \left[ \frac{1}{4} k_\eta(\theta,\varphi) - k_\tau(\theta,\varphi) \right] \cos^4\varphi \sin^2\varphi \sin^6\theta \right] d\varphi \right\} d\theta =$$
$$\mathbb{D}_{111221} = \frac{1}{140} L^4 \left( \frac{1}{4} \bar{k}_\eta - \bar{k}_\tau \right) \tag{54}$$

$$\mathbb{D}_{221122} = \frac{1}{4} L^4 \int_0^\pi \sin\theta \left\{ \int_0^{2\pi} \left[ \left[ \frac{1}{4} k_\eta(\theta,\varphi) - k_\tau(\theta,\varphi) \right] \cos^2\varphi \sin^4\varphi \sin^6\theta \right] d\varphi \right\} d\theta$$
$$+ \frac{1}{4} L^4 \int_0^\pi \sin\theta \left\{ \int_0^{2\pi} \left[ k_\tau(\theta,\varphi) \frac{1}{4} \left[ 2 \left( \cos\varphi \sin\varphi \sin^2\theta \right) \cos\varphi \sin\varphi \sin^2\theta \right] \right] d\varphi \right\} d\theta =$$
$$\mathbb{D}_{221122} = \frac{1}{840} L^4 \left( \frac{3}{2} \bar{k}_\eta + \bar{k}_\tau \right) \tag{55}$$

$$\mathbb{D}_{112223} = \frac{1}{4} L^4 \int_0^\pi \sin\theta \left\{ \int_0^{2\pi} \left[ \left[ \frac{1}{4} k_\eta(\theta,\varphi) - k_\tau(\theta,\varphi) \right] \cos^2\varphi \sin^3\varphi \sin^5\theta \cos\theta \right] d\varphi \right\} d\theta =$$
$$\mathbb{D}_{112223} = \frac{1}{420} L^4 \left( \frac{1}{4} \bar{k}_\eta - \bar{k}_\tau \right) \tag{56}$$

where the isotropic condition has been imposed by assuming no dependence of $k_\eta$ and $k_\tau$ with respect to $\hat{c}$ (or $\theta$ and $\varphi$),

$$k_\tau(\theta,\varphi)=\frac{\bar{k}_\tau}{4\pi},\qquad k_\eta(\theta,\varphi)=\frac{\bar{k}_\eta}{4\pi},$$

where $\bar{k}_\tau$ and $\bar{k}_\eta$ are the new averaged stiffness over the unit sphere $S^2$, that are defined in the general anisotropic case as follows,

$$\bar{k}_\tau=\int_0^{2\pi}\left[\int_0^{\pi}k_\tau(\theta,\varphi)\sin\theta d\theta\right]d\varphi,\qquad \bar{k}_\eta=\int_0^{2\pi}\left[\int_0^{\pi}k_\eta(\theta,\varphi)\sin\theta d\theta\right]d\varphi.$$

It is worth to be noted that positive definiteness of the elastic energy per unit volume for a given grain-pair in (13) is, from (65) and (67) and neglecting the strain gradient contribution the same of (37) but this time is a quadratic form of $G_{11}$, $G_{12}=G_{21}$, $G_{13}=G_{31}$, $G_{22}$, $G_{23}=G_{32}$ and $G_{33}$. Positive condition for the eigenvalues of the Hessian of such a quadratic form, with the insertion of (46), give the same restrictions (38) of the 2D case.

### 4.5 Isotropic micro-macro identification for the 3D case

By comparing (22) and (48) and (50), we obtain

$$\lambda+2\mu=\frac{1}{15}L^2\left(3\bar{k}_\eta+8\bar{k}_\tau\right),\quad \lambda=\frac{1}{15}L^2\left(\bar{k}_\eta-4\bar{k}_\tau\right)$$

that yields an identification of Lamè coefficients that has similarity with that of the 2D case (39) but different expressions, i.e.,

$$\lambda=\frac{1}{15}L^2\left(\bar{k}_\eta-4\bar{k}_\tau\right),\quad \mu=\frac{1}{15}L^2\left(\bar{k}_\eta+6\bar{k}_\tau\right). \tag{57}$$

Thus, in the 3D model Young's modulus $Y_{3D}$ and Poisson's ratio $\nu_{3D}$ are derived in the Appendix 6.2.2 and in (77) in terms of Lamè coefficients as follows, i.e.,

$$Y_{3D}=\mu\frac{3\lambda+2\mu}{\lambda+\mu},\quad \nu_{3D}=\frac{\lambda}{2(\lambda+\mu)}, \tag{58}$$

and vice-versa we have,

$$\lambda=Y_{3D}\frac{\nu_{3D}}{(1+\nu_{3D})(1-2\nu_{3D})},\qquad \mu=Y_{3D}\frac{1}{2(1+\nu_{3D})}.$$

Thus, insertion of (57) into (58) yield, see also [12], the Young's modulus $Y_{3D}$ and Poisson's ratio $\nu_{3D}$ in terms of normal and tangential stiffness,

$$Y_{3D}=\frac{1}{6}L^2\bar{k}_\eta\frac{\bar{k}_\eta+6\bar{k}_\tau}{2\bar{k}_\eta+\bar{k}_\tau},\quad \nu_{3D}=\frac{\bar{k}_\eta-4\bar{k}_\tau}{4\left(\bar{k}_\eta+\bar{k}_\tau\right)}. \tag{59}$$

The inversion of (59) is

$$\bar{k}_\eta=\frac{3Y_{3D}}{L^2(2\nu_{3D}-1)},\quad \bar{k}_\tau=\frac{3Y_{3D}(4\nu_{3D}-1)}{4L^2(2\nu_{3D}-1)(\nu_{3D}+1)}. \tag{60}$$

By comparing $(26)_1$-(52), $(26)_2$-(53), $(27)_1$-(54), $(27)_2$-(55) and $(27)_3$-(56) we obtain

$$\begin{cases}4c_3+c_4+4c_5+2c_6+4c_7=\frac{1}{560}L^4\left(\bar{k}_\eta+8\bar{k}_\tau\right),\\ c_4+2c_6=\frac{1}{1680}L^4\left(3\bar{k}_\eta+16\bar{k}_\tau\right),\\ 2c_3+c_4=\frac{1}{560}L^4\left(\bar{k}_\eta-4\bar{k}_\tau\right),\\ c_3+2c_7=\frac{1}{1680}L^4\left(3\bar{k}_\eta+2\bar{k}_\tau\right),\\ c_3=\frac{1}{1680}L^4\left(\bar{k}_\eta-4\bar{k}_\tau\right),\end{cases}$$

that yields an identification of the 5 isotropic strain gradient coefficients

$$\begin{cases} c_3 = \frac{1}{1680} L^4 \left(\bar{k}_\eta - 4\bar{k}_\tau\right), \\ c_4 = \frac{1}{1680} L^4 \left(\bar{k}_\eta - 4\bar{k}_\tau\right), \\ c_5 = \frac{1}{1680} L^4 \left(\bar{k}_\eta + 3\bar{k}_\tau\right), \\ c_6 = \frac{1}{1680} L^4 \left(\bar{k}_\eta + 10\bar{k}_\tau\right), \\ c_7 = \frac{1}{1680} L^4 \left(\bar{k}_\eta + 3\bar{k}_\tau\right). \end{cases} \tag{61}$$

By assuming the identification in (60) we therefore have,

$$\begin{cases} c_3 = Y_{3D} L^2 \frac{\nu_{3D}}{112(1+\nu_{3D})(1-2\nu_{3D})} = \frac{L^2}{112}\lambda, \\ c_4 = Y_{3D} L^2 \frac{\nu_{3D}}{112(1+\nu_{3D})(1-2\nu_{3D})} = \frac{L^2}{112}\lambda, \\ c_5 = Y_{3D} L^2 \frac{7-8\nu_{3D}}{2240(1+\nu_{3D})(1-2\nu_{3D})} = \frac{L^2}{1120}\left(7\mu + 3\lambda\right) \\ c_6 = Y_{3D} L^2 \frac{7-18\nu_{3D}}{1120(1+\nu_{3D})(1-2\nu_{3D})} = \frac{L^2}{1120}\left(7\mu - 4\lambda\right) \\ c_7 = Y_{3D} L^2 \frac{7-8\nu_{3D}}{2240(1+\nu_{3D})(1-2\nu_{3D})} = \frac{L^2}{1120}\left(7\mu + 3\lambda\right) \end{cases} \tag{62}$$

that means, in terms of the Mindlin's coefficients from (28), we have,

$$\begin{cases} \hat{a}_1 = Y_{3D} L^2 \frac{\nu_{3D}}{56(1+\nu_{3D})(1-2\nu_{3D})} = \frac{L^2}{56}\lambda, \\ \hat{a}_2 = Y_{3D} L^2 \frac{\nu_{3D}}{448(1+\nu_{3D})(1-2\nu_{3D})} = \frac{L^2}{56}\lambda, \\ \hat{a}_3 = Y_{3D} L^2 \frac{7-8\nu_{3D}}{1120(1+\nu_{3D})(1-2\nu_{3D})} = \frac{L^2}{560}\left(7\mu + 3\lambda\right), \\ \hat{a}_4 = Y_{3D} L^2 \frac{7-18\nu_{3D}}{1120(1+\nu_{3D})(1-2\nu_{3D})} = \frac{L^2}{1120}\left(7\mu - 4\lambda\right), \\ \hat{a}_5 = Y_{3D} L^2 \frac{7-8\nu_{3D}}{1120(1+\nu_{3D})(1-2\nu_{3D})} = \frac{L^2}{560}\left(7\mu + 3\lambda\right). \end{cases}$$

It is worth to be noted that the following Aifantis' [4] identification of the 5 strain gradient constitutive parameters

$$c_3 = 0, \quad c_4 = \lambda L^2 = Y_{3D} L^2 \frac{\nu_{3D}}{\left(1+\nu_{3D}\right)\left(1-2\nu_{3D}\right)}, \quad c_5 = 0, \quad c_6 = \mu L^2 = Y_{3D} L^2 \frac{\nu_{3D}}{2\left(1+\nu_{3D}\right)}, \quad c_7 = 0,$$

with a single characteristic length is not compatible with that present in (62). Such expedient simplifications of second gradient elastic parameters, with single characteristic length, can often overlook complete characterization of problems since it is not possible *a priori* to determine what phenomena could be significant in a given case, particularly when considering problems with evolving microstructures [52]. In this regard, it is worth mentioning that even the so-called weak nonlocality assumption is a restricting assumption as pointed out in [36], where it is shown that for transverse isotropy weak nonlocality assumption involving only two independent characteristic lengths fails to describe the different deformations modes of plate bending and a more general consideration is necessary.

## 5 Conclusion

This paper has presented an approach for micro-macro identification of elastic constants of materials with 'microscopic' granular texture. In contrast to previous excursions of similar micro-macro identification, the present work develops the approach in finite deformation framework and considers the contributions of second gradient of placement. In addition, an energy approach is utilized such that clear meanings can be attached to the conjugates of the kinematic measures of relative displacements (needless to say the strain measure and its gradient), and therefore, to the stiffness measures. The key result of this work are the expressions for second-gradient elastic parameters in (41) and (43) for the 2D case and in (59) and (61) for the 3D case in terms of the grain-scale stiffnesses. As a consequence, these expression give an estimate of second-gradient elastic parameters in (44-45) for the 2D case and in (62) for the 3D case in terms of the first gradient parameters (i.e. in terms of the Young's modulus and Poisson's ratio) and a microstructural characteristic length without recourse to *ad hoc* prescriptions or *a priori* (over)simplifications. In these first

estimates the characteristic length is on the order of grain-size. We note, that the approach can be generalized to admit additional grain-scale micro-mechanisms that can lead to more than one characteristic lengths which can be multiples of grain-size of relevance to a material system. These micromechanisms may include those akin to a pantograph, e.g. analyzed in [3, 57, 8], or in plate bending as discussed in [36], or other mechanisms that require additional kinematical descriptors to capture the deformation energy of grain-pair [30, 47, 53, 26]. In these cases, the material can be characterized by multiple elastic characteristic lengths and their derivations will be presented in future works. It is further noted that these elastic parameters that incorporate characteristic lengths have vast applications to practical problems in which classical analyses lead to infinitesimal localizations and other singularities for materials in which microstructure plays a clear role, such as those ranging from natural rocks to woven fabrics.

## Acknowledgement

AM is supported in part by the United States National Science Foundation grant CMMI -1727433.

# 6 Appendix

## 6.1 Derivation of objective relative displacement (16)

The (9) in index notation is

$$u_i^{np} = 2G_{ij}\hat{c}_j L + \frac{1}{2}G_{ij,h}\hat{c}_j\hat{c}_h L^2. \tag{63}$$

Insertion of (63) into (11) yields

$$u_\eta = \frac{1}{2}u_i^{np}\hat{c}_i = LG_{ij}\hat{c}_i\hat{c}_j + \frac{1}{4}L^2 G_{ij,h}\hat{c}_i\hat{c}_j\hat{c}_h. \tag{64}$$

Its square is

$$u_\eta^2 = \left(LG_{ij}\hat{c}_i\hat{c}_j + \frac{1}{4}L^2 G_{ij,h}\hat{c}_i\hat{c}_j\hat{c}_h\right)\left(LG_{ab}\hat{c}_a\hat{c}_b + \frac{1}{4}L^2 G_{ab,c}\hat{c}_a\hat{c}_b\hat{c}_c\right)$$

or

$$u_\eta^2 = L^2\hat{c}_i\hat{c}_j\hat{c}_a\hat{c}_b G_{ij}G_{ab} + \frac{1}{2}L^3\hat{c}_i\hat{c}_j\hat{c}_a\hat{c}_b\hat{c}_c G_{ij}G_{ab,c} + \frac{1}{16}L^4\hat{c}_i\hat{c}_j\hat{c}_h\hat{c}_a\hat{c}_b\hat{c}_c G_{ij,h}G_{ab,c}. \tag{65}$$

Insertion of (63) into (12) yields

$$u_\tau^2 = \left(u^{np} - \left(u^{np}\cdot\hat{c}\right)\hat{c}\right)\cdot\left(u^{np} - \left(u^{np}\cdot\hat{c}\right)\hat{c}\right) = u^{np}\cdot u^{np} - \left(u^{np}\cdot\hat{c}\right)^2 \tag{66}$$

or, in index notation,

$$u_\tau^2 = \left(2G_{ij}\hat{c}_j L + \frac{1}{2}G_{ij,h}\hat{c}_j\hat{c}_h L^2\right)\left(2G_{ik}\hat{c}_k L + \frac{1}{2}G_{im,n}\hat{c}_m\hat{c}_n L^2\right) - 4u_\eta^2,$$

that means

$$u_\tau^2 + 4u_\eta^2 = 4L^2 G_{ij}G_{ik}\hat{c}_j\hat{c}_k + 2L^3 G_{ij}G_{im,n}\hat{c}_j\hat{c}_m\hat{c}_n + \frac{1}{4}L^4 G_{ij,h}G_{im,n}\hat{c}_j\hat{c}_h\hat{c}_m\hat{c}_n$$

or, taking (65) into account,

$$\begin{aligned} u_\tau^2 &= 4L^2 G_{ij}G_{ab}\left(\delta_{ia}\hat{c}_j\hat{c}_b - \hat{c}_i\hat{c}_j\hat{c}_a\hat{c}_b\right) + 2L^3 G_{ij}G_{ab,c}\left(\delta_{ia}\hat{c}_j\hat{c}_b\hat{c}_c - \hat{c}_i\hat{c}_j\hat{c}_a\hat{c}_b\hat{c}_c\right) \\ &+ \frac{1}{4}L^4 G_{ij,h}G_{am,n}\left(\delta_{ia}\hat{c}_j\hat{c}_h\hat{c}_m\hat{c}_n - \hat{c}_i\hat{c}_j\hat{c}_h\hat{c}_a\hat{c}_b\hat{c}_c\right). \end{aligned} \tag{67}$$

## 6.2 Derivation of Young modulus and Poisson's ratio in the 2D and 3D cases

By assuming horizontal $u_1$ and vertical $u_2$ affine displacement fields and the following constant external actions along the horizontal and vertical directions,

$$u_1 = \alpha X_1, \quad u_2 = \beta X_2, \quad S\mathbf{e}_1 = F, \quad S\mathbf{e}_2 = 0, \tag{68}$$

we define Young modulus $Y$ and Poisson ratio $\nu$,

$$Y = \frac{F}{E_{11}}, \quad \nu = -\frac{E_{22}}{E_{11}},$$

where the Piola stress tensor $S$ is defined

$$S = \frac{\partial U}{\partial G} = 2\mu G + \lambda \mathrm{Tr} G \cong 2\mu E + \lambda \mathrm{Tr} E \tag{69}$$

for small deformation

$$G \cong E = \frac{1}{2}\left[\nabla u + (\nabla u)^T\right]. \tag{70}$$

Thus, Young modulus $Y$ and Poisson ratio $\nu$ are linked with the external action $F$ and to the components $\alpha$ and $\beta$ of the deformation

$$Y = \frac{F}{\alpha}, \quad \nu = -\frac{\beta}{\alpha}. \tag{71}$$

### 6.2.1 The 2D case

In the $2D$ case, from strain (70), displacement (68) and stress (69) definitions, we have

$$E = \begin{pmatrix} \alpha & 0 \\ 0 & \beta \end{pmatrix}, \quad \mathrm{Tr} E = \alpha + \beta, \quad S = \begin{pmatrix} 2\mu\alpha + \lambda(\alpha+\beta) & 0 \\ 0 & 2\mu\beta + \lambda(\alpha+\beta) \end{pmatrix}. \tag{72}$$

By insertion of (72) into (68) we obtain the relation between the deformation components $\alpha$ and $\beta$,

$$\begin{cases} S\mathbf{e}_1 = F = 2\mu\alpha + \lambda(\alpha+\beta) \\ S\mathbf{e}_2 = 0 = 2\mu\beta + \lambda(\alpha+\beta) \end{cases} \Rightarrow \quad \beta = -\frac{\lambda\alpha}{\lambda+2\mu}, \tag{73}$$

that gives, by insertion of (73) into (71), the relation between Young modulus $Y$ and Poisson ratio $\nu$ with Lamè coefficients in the $2D$ case,

$$Y_{2D} = \frac{F}{\alpha} = 2\mu + \lambda\left(1 - \frac{\lambda}{\lambda+2\mu}\right) = \frac{(\lambda+2\mu)^2 - \lambda^2}{\lambda+2\mu} = 4\mu\frac{\lambda+\mu}{\lambda+2\mu}, \quad \nu_{2D} = -\frac{\beta}{\alpha} = \frac{\lambda}{\lambda+2\mu} \tag{74}$$

### 6.2.2 The 3D case

In the $3D$ case we further assume, for the third direction, the same behavior of the vertical direction of the $2D$ case

$$u_3 = \beta X_2, \quad S\mathbf{e}_3 = 0, \tag{75}$$

so that strain and stress are modified as follows

$$E = \begin{pmatrix} \alpha & 0 & 0 \\ 0 & \beta & 0 \\ 0 & 0 & \beta \end{pmatrix}, \quad \mathrm{Tr} E = \alpha + 2\beta, \quad S = \begin{pmatrix} 2\mu\alpha + \lambda(\alpha+2\beta) & 0 & 0 \\ 0 & 2\mu\beta + \lambda(\alpha+2\beta) & 0 \\ 0 & 0 & 2\mu\beta + \lambda(\alpha+2\beta) \end{pmatrix}$$

and the relation between the deformation components $\alpha$ and $\beta$ are different

$$\begin{cases} S\mathbf{e}_1 = F = 2\mu\alpha + \lambda(\alpha+2\beta) \\ S\mathbf{e}_2 = 0 = 2\mu\beta + \lambda(\alpha+2\beta) \end{cases} \Rightarrow \quad \beta = -\frac{\lambda\alpha}{2(\lambda+\mu)}, \tag{76}$$

and different is relation between Young modulus $Y$ and Poisson ratio $\nu$ with Lamè coefficients,

$$Y_{3D} = \frac{F}{\alpha} = 2\mu + \lambda\left(1 - \frac{\lambda}{\lambda+\mu}\right) = \frac{(\lambda+2\mu)(\lambda+\mu) - \lambda^2}{\lambda+\mu} = \mu\frac{3\lambda+2\mu}{\lambda+2\mu}, \quad \nu_{3D} = -\frac{\beta}{\alpha} = \frac{\lambda}{2(\lambda+\mu)}. \tag{77}$$

# References


[1] B.E. Abali, W.H. Müller, and F. dell'Isola. Theory and computation of higher gradient elasticity theories based on action principles. *Archive of Applied Mechanics*, pages 1–16, 2017.

[2] B.E. Abali, W.H. Müller, and V.A. Eremeyev. Strain gradient elasticity with geometric nonlinearities and its computational evaluation. *Mechanics of Advanced Materials and Modern Processes*, 1(1):4, 2015.

[3] J-J. Alibert, P. Seppecher, and F. dell'Isola. Truss modular beams with deformation energy depending on higher displacement gradients. *Mathematics and Mechanics of Solids*, 8(1):51–73, 2003.

[4] BS Altan and EC Aifantis. On some aspects in the special theory of gradient elasticity. *Journal of the Mechanical Behavior of Materials*, 8(3):231–282, 1997.

[5] U. Andreaus, F. dell'Isola, I. Giorgio, L. Placidi, T. Lekszycki, and N.L. Rizzi. Numerical simulations of classical problems in two-dimensional (non) linear second gradient elasticity. *International Journal of Engineering Science*, 108:34–50, 2016.

[6] N. Auffray, F. dell'Isola, V. Eremeyev, A. Madeo, and G. Rosi. Analytical continuum mechanics à la Hamilton–Piola least action principle for second gradient continua and capillary fluids. *Mathematics and Mechanics of Solids*, 20(4):375–417, 2015.

[7] N. Auffray, J. Dirrenberger, and G. Rosi. A complete description of bi-dimensional anisotropic strain-gradient elasticity. *International Journal of Solids and Structures*, 69:195–206, 2015.

[8] Patrick Auger, Thomas Lavigne, Benjamin Smaniotto, Mario Spagnuolo, Francesco dell'Isola, and FranÃ§ois Hild. Poynting effects in pantographic metamaterial captured via multiscale dvc. *The Journal of Strain Analysis for Engineering Design*, 0(0), 2020.

[9] C. Boutin, I. Giorgio, L. Placidi, et al. Linear pantographic sheets: Asymptotic micro-macro models identification. *Mathematics and Mechanics of Complex Systems*, 5(2):127–162, 2017.

[10] C. Caggegi, N. Pensée, M. Fagone, M. Cuomo, and L. Chevalier. Experimental global analysis of the efficiency of carbon fiber anchors applied over cfrp strengthened bricks. *Construction and Building Materials*, 53:203–212, 2014.

[11] J. Cao, R. Akkerman, P. Boisse, J. Chen, et al. Characterization of mechanical behavior of woven fabrics: experimental methods and benchmark results. *Composites Part A: Applied Science and Manufacturing*, 39(6):1037–1053, 2008.

[12] Antonio Cazzani and Marco Rovati. Extrema of Young's modulus for cubic and transversely isotropic solids. *International Journal of Solids and Structures*, 40(7):1713–1744, 2003.

[13] Ching S Chang and Jian Gao. Second-gradient constitutive theory for granular material with random packing structure. *International Journal of Solids and Structures*, 32(16):2279–2293, 1995.

[14] Ching S Chang and Anil Misra. Packing structure and mechanical properties of granulates. *Journal of engineering mechanics*, 116(5):1077–1093, 1990.

[15] Nicolas M Cordero, Samuel Forest, and Esteban P Busso. Second strain gradient elasticity of nano-objects. *Journal of the Mechanics and Physics of Solids*, 97:92–124, 2016.

[16] M. Cuomo, F. dell'Isola, L. Greco, and N.L. Rizzi. First versus second gradient energies for planar sheets with two families of inextensible fibres: Investigation on deformation boundary layers, discontinuities and geometrical instabilities. *Composites Part B: Engineering*, 2016.

[17] F. dell'Isola, M. Cuomo, L. Greco, and A. Della Corte. Bias extension test for pantographic sheets: numerical simulations based on second gradient shear energies. *Journal of Engineering Mathematics*, pages 1–31, 2016.

[18] F. dell'Isola, A. Della Corte, and I. Giorgio. Higher-gradient continua: The legacy of Piola, Mindlin, Sedov and Toupin and some future research perspectives. *Mathematics and Mechanics of Solids*, page 1081286515616034, 2016.

[19] F. dell'Isola and I. Giorgio. Large deformations of planar extensible beams and pantographic lattices: heuristic homogenization, experimental and numerical examples of equilibrium. *Proc. R. Soc. A*, 472(2185):20150790, 2016.

[20] F. dell'Isola, I. Giorgio, and U. Andreaus. Elastic pantographic 2d lattices: a numerical analysis on static response and wave propagation. In *Proceedings of the Estonian Academy of Sciences*, volume 64, pages 219–225, 2015.

[21] Francesco dell'Isola, Giulio Sciarra, and Stefano Vidoli. Generalized hooke's law for isotropic second gradient materials. *Proceedings of the Royal Society A: Mathematical, Physical and Engineering Sciences*, 465(2107):2177–2196, 2009.

[22] V. A Eremeyev, F. dell'Isola, C. Boutin, and D. Steigmann. Linear pantographic sheets: existence and uniqueness of weak solutions. 2017.

[23] Victor A Eremeyev and Holm Altenbach. Equilibrium of a second-gradient fluid and an elastic solid with surface stresses. *Meccanica*, 49(11):2635–2643, 2014.

[24] Victor A Eremeyev and Holm Altenbach. On the direct approach in the theory of second gradient plates. In *Shell and Membrane Theories in Mechanics and Biology*, pages 147–154. Springer, 2015.

[25] Manuel Ferretti, Angela Madeo, Francesco dell'Isola, and Philippe Boisse. Modeling the onset of shear boundary layers in fibrous composite reinforcements by second-gradient theory. *Zeitschrift für angewandte Mathematik und Physik*, 65(3):587–612, 2014.

[26] Patrick Franciosi and Mario Spagnuolo. Homogenization-Based Mechanical Behavior Modeling of Composites Using Mean Green Operators for Infinite Inclusion Patterns or Networks Possibly Co-continuous with a Matrix. In *F. dell'Isola, L. Igumnov (Eds). Dynamics, Strength of Materials and Durability in Multiscale Mechanics*, pages 245–280. Springer, 2021.

[27] I. Giorgio. Numerical identification procedure between a micro-Cauchy model and a macro-second gradient model for planar pantographic structures. *Zeitschrift für angewandte Mathematik und Physik*, 67(4)(95), 2016.

[28] I. Giorgio, A. Della Corte, and F. dell'Isola. Dynamics of 1D nonlinear pantographic continua. *Nonlinear Dynamics*, 88(1):21–31, 2017.

[29] I Giorgio, P Harrison, F dell'Isola, J Alsayednoor, and E Turco. Wrinkling in engineering fabrics: a comparison between two different comprehensive modelling approaches. *Proceedings of the Royal Society A: Mathematical, Physical and Engineering Sciences*, 474(2216), 2018.

[30] Ivan Giorgio, Francesco dell'Isola, and Anil Misra. Chirality in 2D cosserat media related to stretch-micro-rotation coupling with links to granular micromechanics. *International Journal of Solids and Structures*, 202:28–38, 2020.

[31] L. Greco, I. Giorgio, and A. Battista. In plane shear and bending for first gradient inextesible pantographic sheets: numerical study of deformed shapes and global constraint reactions. *Mathematics and Mechanics of Solids*, page 1081286516651324, 2016.

[32] J Jenkins, D Johnson, L La Ragione, and H Makse. Fluctuations and the effective moduli of an isotropic, random aggregate of identical, frictionless spheres. *Journal of the Mechanics and Physics of Solids*, 53(1):197–225, 2005.

[33] Sergei Khakalo, Viacheslav Balobanov, and Jarkko Niiranen. Modelling size-dependent bending, buckling and vibrations of 2d triangular lattices by strain gradient elasticity models: applications to sandwich beams and auxetics. *International Journal of Engineering Science*, 127:33–52, 2018.

[34] Sergei Khakalo and Jarkko Niiranen. Form ii of mindlin's second strain gradient theory of elasticity with a simplification: For materials and structures from nano-to macro-scales. *European Journal of Mechanics-A/Solids*, 71:292–319, 2018.

[35] Sergei Khakalo and Jarkko Niiranen. Lattice structures as thermoelastic strain gradient metamaterials: Evidence from full-field simulations and applications to functionally step-wise-graded beams. *Composites Part B: Engineering*, 177:107224, 2019.

[36] Sergei Khakalo and Jarkko Niiranen. Anisotropic strain gradient thermoelasticity for cellular structures: Plate models, homogenization and isogeometric analysis. *Journal of the Mechanics and Physics of Solids*, 134:103728, 2020.

[37] N Korshunova, G Alaimo, SB Hosseini, M Carraturo, A Reali, J Niiranen, F Auricchio, E Rank, and S Kollmannsberger. Bending behavior of octet-truss lattice structures: modelling options, numerical characterization and experimental validation. *submitted to Materials & Design*, 2021.

[38] David CC Lam, Fan Yang, ACM Chong, Jianxun Wang, and Pin Tong. Experiments and theory in strain gradient elasticity. *Journal of the Mechanics and Physics of Solids*, 51(8):1477–1508, 2003.

[39] Markus Lazar, Gérard A Maugin, and Elias C Aifantis. Dislocations in second strain gradient elasticity. *International Journal of Solids and Structures*, 43(6):1787–1817, 2006.

[40] Angela Madeo, Francesco dell'Isola, and Félix Darve. A continuum model for deformable, second gradient porous media partially saturated with compressible fluids. *Journal of the Mechanics and Physics of Solids*, 61(11):2196–2211, 2013.

[41] Holger A Meier, Paul Steinmann, and Ellen Kuhl. Towards multiscale computation of confined granular media. *Technische Mechanik-European Journal of Engineering Mechanics*, 28(1):32–42, 2008.

[42] Raymond David Mindlin. Second gradient of strain and surface-tension in linear elasticity. *International Journal of Solids and Structures*, 1(4):417–438, 1965.

[43] R.D. Mindlin and N.N. Eshel. On first strain-gradient theories in linear elasticity. *International Journal of Solids and Structures*, 4(1):109 – 124, 1968.

[44] Anil Misra and Ching S Chang. Effective elastic moduli of heterogeneous granular solids. *International Journal of Solids and Structures*, 30(18):2547–2566, 1993.

[45] Anil Misra, Nima Nejadsadeghi, Michele De Angelo, and Luca Placidi. Chiral metamaterial predicted by granular micromechanics: verified with 1D example synthesized using additive manufacturing. *Continuum Mechanics and Thermodynamics*, pages 1–17, 2020.

[46] Anil Misra and Payam Poorsolhjouy. Identification of higher-order elastic constants for grain assemblies based upon granular micromechanics. *Mathematics and Mechanics of Complex Systems*, 3(3):285–308, 2015.

[47] Nima Nejadsadeghi and Anil Misra. Extended granular micromechanics approach: a micromorphic theory of degree n. *Mathematics and Mechanics of Solids*, 25(2):407–429, 2020.

[48] R.W. Ogden. Large deformation isotropic elasticity-on the correlation of theory and experiment for incompressible rubberlike solids. In *Proceedings of the Royal Society of London A: Mathematical, Physical and Engineering Sciences*, volume 326, pages 565–584. The Royal Society, 1972.

[49] Catherine Pideri and Pierre Seppecher. A second gradient material resulting from the homogenization of an heterogeneous linear elastic medium. *Continuum Mechanics and Thermodynamics*, 9(5):241–257, 1997.

[50] L. Placidi, U. Andreaus, A. Della Corte, and T. Lekszycki. Gedanken experiments for the determination of two-dimensional linear second gradient elasticity coefficients. *Zeitschrift für angewandte Mathematik und Physik*, 66(6):3699–3725, 2015.

[51] L. Placidi, U. Andreaus, and I. Giorgio. Identification of two-dimensional pantographic structure via a linear d4 orthotropic second gradient elastic model. *Journal of Engineering Mathematics*, pages 1–21, 2016.

[52] Luca Placidi, Anil Misra, and Emilio Barchiesi. Simulation results for damage with evolving microstructure and growing strain gradient moduli. *Continuum Mechanics and Thermodynamics*, 31(4):1143–1163, 2019.

[53] Payam Poorsolhjouy and Anil Misra. Granular micromechanics based continuum model for grain rotations and grain rotation waves. *Journal of the Mechanics and Physics of Solids*, 129:244–260, 2019.

[54] Y. Rahali, I. Giorgio, J.F. Ganghoffer, and F. dell'Isola. Homogenization à la Piola produces second gradient continuum models for linear pantographic lattices. *International Journal of Engineering Science*, 97:148–172, 2015.

[55] J.C. Reiher, I. Giorgio, and A. Bertram. Finite-element analysis of polyhedra under point and line forces in second-strain gradient elasticity. *Journal of Engineering Mechanics*, 143(2):04016112, 2016.

[56] G. Sciarra, F. dell'Isola, and O. Coussy. Second gradient poromechanics. *International Journal of Solids and Structures*, 44(20):6607–6629, 2007.

[57] P. Seppecher, J.-J. Alibert, and F. dell'Isola. Linear elastic trusses leading to continua with exotic mechanical interactions. In *Journal of Physics: Conference Series*, volume 319, page 012018. IOP Publishing, 2011.

[58] M. Spagnuolo, K. Barcz, A. Pfaff, F. dell'Isola, and P. Franciosi. Qualitative pivot damage analysis in aluminum printed pantographic sheets: numerics and experiments. *Mechanics Research Communications*, 2017.

[59] Paul Steinmann, A Elizondo, and R Sunyk. Studies of validity of the Cauchy–Born rule by direct comparison of continuum and atomistic modelling. *Modelling and Simulation in Materials Science and Engineering*, 15(1):S271, 2006.

[60] Jalal Torabi and Jarkko Niiranen. Microarchitecture-dependent nonlinear bending analysis for cellular plates with prismatic corrugated cores via an anisotropic strain gradient plate theory of first-order shear deformation. *Engineering Structures*, 236:112117, 2021.

[61] Loc V Tran and Jarkko Niiranen. A geometrically nonlinear euler–bernoulli beam model within strain gradient elasticity with isogeometric analysis and lattice structure applications. *Mathematics and Mechanics of Complex Systems*, 8(4):345–371, 2020.

[62] Emilio Turco, Francesco dell'Isola, and Anil Misra. A nonlinear lagrangian particle model for grains assemblies including grain relative rotations. *International Journal for Numerical and Analytical Methods in Geomechanics*, 43(5):1051–1079, 2019.

[63] K Walton. The effective elastic moduli of a random packing of spheres. *Journal of the Mechanics and Physics of Solids*, 35(2):213–226, 1987.

[64] FACM Yang, ACM Chong, David Chuen Chun Lam, and Pin Tong. Couple stress based strain gradient theory for elasticity. *International journal of solids and structures*, 39(10):2731–2743, 2002.

[65] Hua Yang, Bilen Emek Abali, Dmitry Timofeev, and Wolfgang H Müller. Determination of metamaterial parameters by means of a homogenization approach based on asymptotic analysis. *Continuum Mechanics and Thermodynamics*, pages 1–20, 2019.

[66] Hua Yang, Dmitry Timofeev, Ivan Giorgio, and Wolfgang H Müller. Effective strain gradient continuum model of metamaterials and size effects analysis. *Continuum Mechanics and Thermodynamics*, pages 1–23, 2020.